CEA/SACLAY
DSM

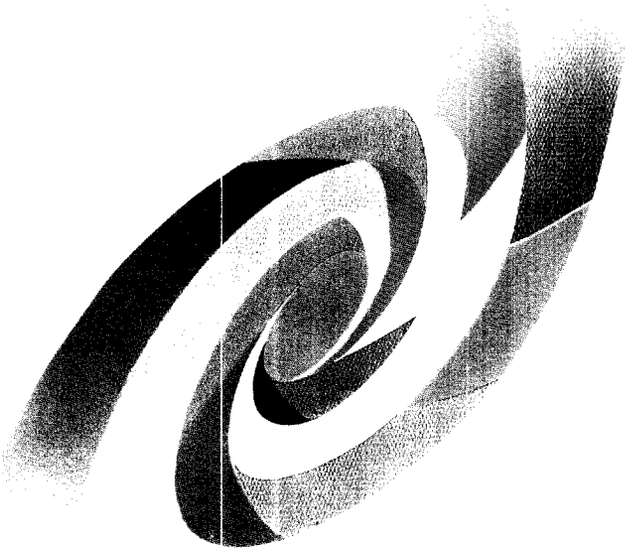

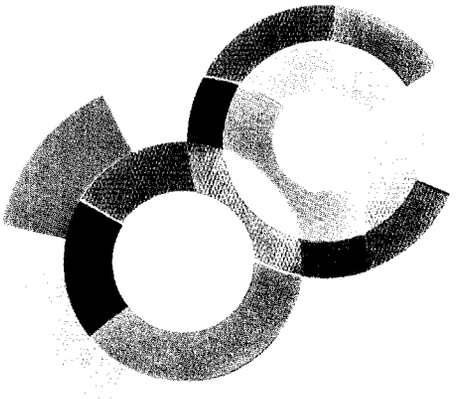

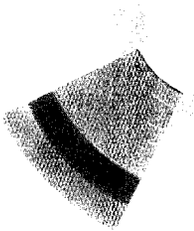

DAPNIA/SPhN-98-09 02/1998

Inelastic proton scattering and nuclear structure towards the drip lines

DAPNIA

N. Alamanos, F. Auger, B.A. Brown and A. Pakou

Département d'**A**strophysique, de Physique des **P**articules, de Physique **N**ucléaire et de l'**I**nstrumentation **A**ssociée
CEA/Saclay F-91191 Gif-sur-Yvette Cédex

Couverture Sylvie Cabrit et Marc Sauvage

International Workshop on Physics with
Radioactive Nuclear Beams,
PURI (Inde), January 12-17, 1998

INELASTIC PROTON SCATTERING AND NUCLEAR STRUCTURE TOWARDS THE DRIP LINES

N. Alamanos[1], F. Auger[1], B.A. Brown[2] and A. Pakou[1,3]

1) DAPNIA/SPhN, CEA/Saclay, 91191 Gif-sur-Yvette Cedex, France
2) National Superconducting Cyclotron Laboratory, Michigan State University, East Lansing, Michigan 48824, U.S.A.
3) Department of Physics, The University of Ioannina, 451 10 Ioannina, Greece

The determination of transition matrix elements by inelastic proton scattering, for $0^+ \rightarrow 2^+$ transitions, is investigated in the context of a microscopic description. Calculations are performed for ^{32}S and the exotic nucleus ^{38}S. The change of the valence shell model effective charges is investigated when moving from the sd ^{32}S nucleus to ^{38}S. It is shown that by proton inelastic scattering it is possible to study the shell model structure for unstable nuclei.

Proton and neutron inelastic scattering are very powerful tools for nuclear structure studies, since strongly collective states are preferentially excited by these probes. The isospin composition of these excitations may be investigated through a comparison of proton and neutron inelastic scattering or alternatively by comparison of proton or neutron inelastic scattering and electromagnetic excitation measurements.

Deviations from the hydrodynamic equality between proton and neutron deformations have been well established in the past, for single closed stable nuclei [1-2]. With the advent of radioactive beam facilities, it has become possible to measure neutron and proton multipole transition matrix elements M_n, M_p and investigate the evolution of nuclear structure when moving towards the drip lines. The neutron and proton transition matrix elements are given by the relation :

$$M^{\lambda}_{n,(p)} = \int \rho^{n(p)}_{tr,\lambda} r^{\lambda+2} dr \qquad (1)$$

where $\rho_{tr}^{n(p)}$ are the neutron (proton) transition densities and λ the multipolatity of the transition.

Proton inelastic scattering data with unstable beams are rather scarce. The doubly magic nucleus ^{56}Ni [3] and the unstable two neutron halo nucleus ^{11}Li [4] were studied by (p,p') scattering in inverse kinematics. Recently elastic and inelastic proton scattering on the unstable ^{38}S nucleus was also reported [5]. Since for S isotopes the excitation energies and the B(E2) values of the first 2^+ states have been also measured through coulomb excitation by T. Glasmacher et al. [6], it was tempting to extract for ^{38}S the M_n/M_p ratio in order to study the evolution of the nuclear structure for nuclei approaching the drip lines. This analysis was performed by J.H. Kelley et al. [5], using an empirical formula established some years ego by Bernstein et al. [2], for λ=2 and 3^- transitions.

$$\frac{M_n}{M_p} = \frac{b_p^p}{b_n^p}\left[\frac{\delta_N}{\delta_{em}}\left(1+\frac{b_n^p}{b_p^p}\frac{N}{Z}\right)-1\right] \qquad (2)$$

where b_p^p and b_n^p are the proton-proton and proton-neutron interaction strengths and δ the usual deformation parameters for nuclear excitations δ_N and electromagnetic excitation δ_{em}. To extract the nuclear deformation length, the angular distributions of scattered protons are generally analyzed using the distorted wave Born approximation or coupled channels with a form factor which assumes either vibrational or rotational behavior. The optical potentials needed to generate the entrance and exit channel distorted waves are usually taken from the global analysis of Becchetti and Greenless and are of Woods-Saxon type [7]. The extracted M_n/M_p ratios for ^{32,34,36,38}S are presented in Table 1. The M_n/M_p ratio for ^{38}S is of the order of 2.1 indicating a significant isovector contribution to the 2^+ state. However, it is well known that this prescription suffers from ambiguities and must be calibrated for each multipolarity using known transitions in nearby nuclei [8]. The validity of this prescription is even more uncertain in the case of unstable nuclei were often the neutron and proton density and concomitantly the corresponding potentials have different root mean square radii.

In this contribution we present calculations of elastic and inelastic scattering cross sections in a microscopic DWBA approach, in which entrance- and exit-channel optical potentials as well as transition form factors are calculated

consistently in a folding model using an energy and density dependent interaction. derived from the nuclear matter calculation of Jeukenne, Lejeune and Mahaux [9], [10]. The proton and neutron ground state density and transition densities used in the folding integrals were obtained from shell model calculations.

From the valence shell model point of view the proton and neutron multipole matrix elements M_p, M_n are constructed from the valence matrix elements A_p and A_n by :

$$M_p = \left(1 + C_{pp}\right)A_p + C_{pn}A_n \qquad (3)$$

$$M_n = C_{np}A_p + \left(1 + C_{nn}\right)A_n$$

where C_{cv} are the generalized effective charges due to polarization of the core (c) nucleons by the valence (v) nucleons [11]. For the sd shell nuclei when both protons and neutrons are in the same valence shell it is a good approximation to assume that $C_{pp}= C_{nn}$ and $C_{np}= C_{pn}$. For these nuclei the experimental data are consistent with an average value of the generalized effective charges of 0.35 although some fluctuations do exist [11].

In Fig.1 the theoretical transition density for the excitation of the 2^+ state of ^{32}S is compared to the experimental transition density distribution obtained from electron inelastic scattering experiments [12]. The good agreement between theory and the experimental results gives confidence in the ability of the shell model code to compute realistic density distributions.

The analysis within our folding model of the elastic and inelastic scattering data on ^{32}S measured by Fabrici et al. [13] provided a M_n/M_p ratio of the order of 1.0, which is the expected value in the limit where the neutron and proton deformations are the same and N=Z as this is the case for ^{32}S [5,7], see Table1. This result supports the quantitative accuracy of this method to reproduce inelastic scattering angular distributions with meaningful multipole transition matrix elements.

For nuclei like ^{38}S where the protons and neutrons are in different valence orbits the generalized effective charges may be different. Indeed, to fit the $B(E2)=|M_p|^2 = 245.3\ e^2fm^4$ value for ^{38}S obtained by the electromagnetic excitation measurements by T. Glasmacher et al. [6], it was necessary to modify the effective charges. A good agreement with the experimental results was obtained assuming

$C_{pp}= C_{nn}=0.35$ and $C_{pn} = C_{np} =0.65$, where $C_{pp}=0.35$ is the usual sd-shell value. For ^{38}S the C_{pn} is larger than C_{pp} because in these shell model calculations the neutron valence space was truncated to include only the $p_{3/2}$ and $f_{7/2}$ shell so that the effective charge has to account for the $p_{3/2}$ to $f_{5/2}$, $p_{3/2}$ to $p_{1/2}$ and $f_{7/2}$ to $f_{5/2}$ transitions and because the overall effective charge in the fp shell may be larger, due to the larger size of the valence fp orbits relative to the size of the sd orbits. With these new values of the generalized effective charges and with $A_p= 5.42$ and $A_n= 12.84$, obtained by using harmonic oscillator wave functions, we obtain from equation (3) $M_n/M_p=1.33$.

In Fig. 2 and 3 angular distributions for the ground state and the 2^+ state in the $^{38}S(p,p')$ reaction at 39MeV/nucleon are presented. With the data, folding model calculations for elastic and inelastic scattering are also presented. The ^{38}S neutron and proton density for the entrance channel potential and transition form factor calculations were also provided by shell model calculations, with $M_n/M_p=1.33$. The central optical potential was modified by the introduction of a multiplicative normalization parameter λ_w for the imaginary potential. This parameter was varied smoothly up to $\lambda_w =0.8$ to best reproduce the elastic scattering experimental cross section shown in Fig. 2. The same re-normalization of the entrance channel optical potential was assumed in the inelastic scattering calculations. The inelastic scattering angular distribution data in Fig. 3, is rather underestimated by our calculations, indicating that the assumed M_n/M_p ratio is not adequate for ^{38}S. However, since Mp was obtained from electromagnetic excitation measurements, the only unknown quantity in this (p,p') inelastic scattering measurement is M_n (or the ratio M_n/M_p). In order to fit the inelastic proton data, the ratio of the multipole matrix elements had to be changed to $M_n/M_p=1.58$, which corresponds to an effective neutron charge of $C_{nn}=0.65$. This increase of the value of C_{nn} from 0.35 to 0.65 may also be related to the truncation in the orbitals used for neutrons. With this new value of the effective neutron charge we obtain a rather reasonable agreement with the experimental results. However, the M_n/M_p obtained by our folding model calculations is rather different to the value obtained by J.H. Kelley et al. [5] by applying the prescription of Bernstein, Table 1. The origin of this difference is probably related to the fact that ^{38}S develops an extended neutron skin. This is shown in Fig. 4 where the ground state and transition density distributions for both

protons and neutrons are shown. In view of these differences between the proton and neutron density distribution we can speculate that the use of an average phenomenological potential of Woods-Saxon form to describe elastic and inelastic scattering is not any more justified, see also eq. (1.4) and (1.5) in [10].

In this letter we have presented the analysis of proton elastic and inelastic scattering on ^{32}S and ^{38}S with a microscopic folding model using an energy- and density-dependent effective interaction and shell model ground state and transition densities. Within this model it was possible to investigate the change of the generalized effective charges for the fd ^{38}S unstable nucleus.

Acknowledgments

The authors would like to thank Pr. K. Kemper for many enlightening discussions and for his careful reading of the manuscript. We would like to thank also Dr. V. Lapoux for her interest in this work and for a careful reading of the manuscript.

References

[1] A. M. Bernstein, V. R. Brown and V. A. Madsen, Phys. Lett. 103B (1981) 255 .

[2] A. M. Bernstein, V. R. Brown, V. A . Madsen, Comments Nucl. Part. Phys. 11 (1983) 203

[3] G. Kraus et al., Phys. Rev. Lett. 73 (1995) 1773.

[4] A.A. Korsheninnikov et al., Phys. Rev. Lett. 78 (1994) 2317.

[5] J.H. Kelley et al., Phys. Rev. C56 (1997) R1206.

[6] T. Glasmacher et al., Phys. Lett. B395 (1997) 163.

[7] M.A. Kennedy et al., Phys. Rev. C46 (1992) 1811.

[8] M.A. Khandaker et al., Phys. Rev. C44 (1991) 1978.

[9] J.P. Jeukenne et al., Phys. Rev. C16 (1977) 80, and references therein

[10] N. Alamanos and P. Roussel-Chomaz, Ann. Phys. Fr. 21 (1996) 601 and references therein.

[11] B.A Brown et al., Phys. Rep. 5 (1983) 313.

[12] J.J. Kelly et al., Phys. Rev. C44 (1991) 1963.

[13] Fabrici et al, Phys. Rev. C 21 (1980) 830.

Figure captions

1) Transition density distributions for the first 2^+ state of ^{32}S. The solid line corresponds to the experimental results obtained by inelastic electron scattering and the dotted line to the shell model calculations.

2) Angular distribution for the $^{38}S(p,p)$ elastic scattering measured at 39MeV/u. The solid line corresponds to folding model calculations.

3) Angular distribution for the $^{38}S(p,p')$ inelastic scattering measured at 39MeV/u. The calculations correspond to two different hypothesis for the shell model generalized effective charges.

4) Neutron and proton ground state and transition density distributions for ^{38}S, corresponding to the multipole matrix elements which reproduce the experimental results.

	E_x (MeV) (experimental)	M_n/M_p from [5]	M_n/M_p this work
^{32}S	2.23	0.84	1.00
^{34}S	2.12	1.26	--
^{36}S	3.29	1.40	--
^{38}S	1.29	2.06	1.58

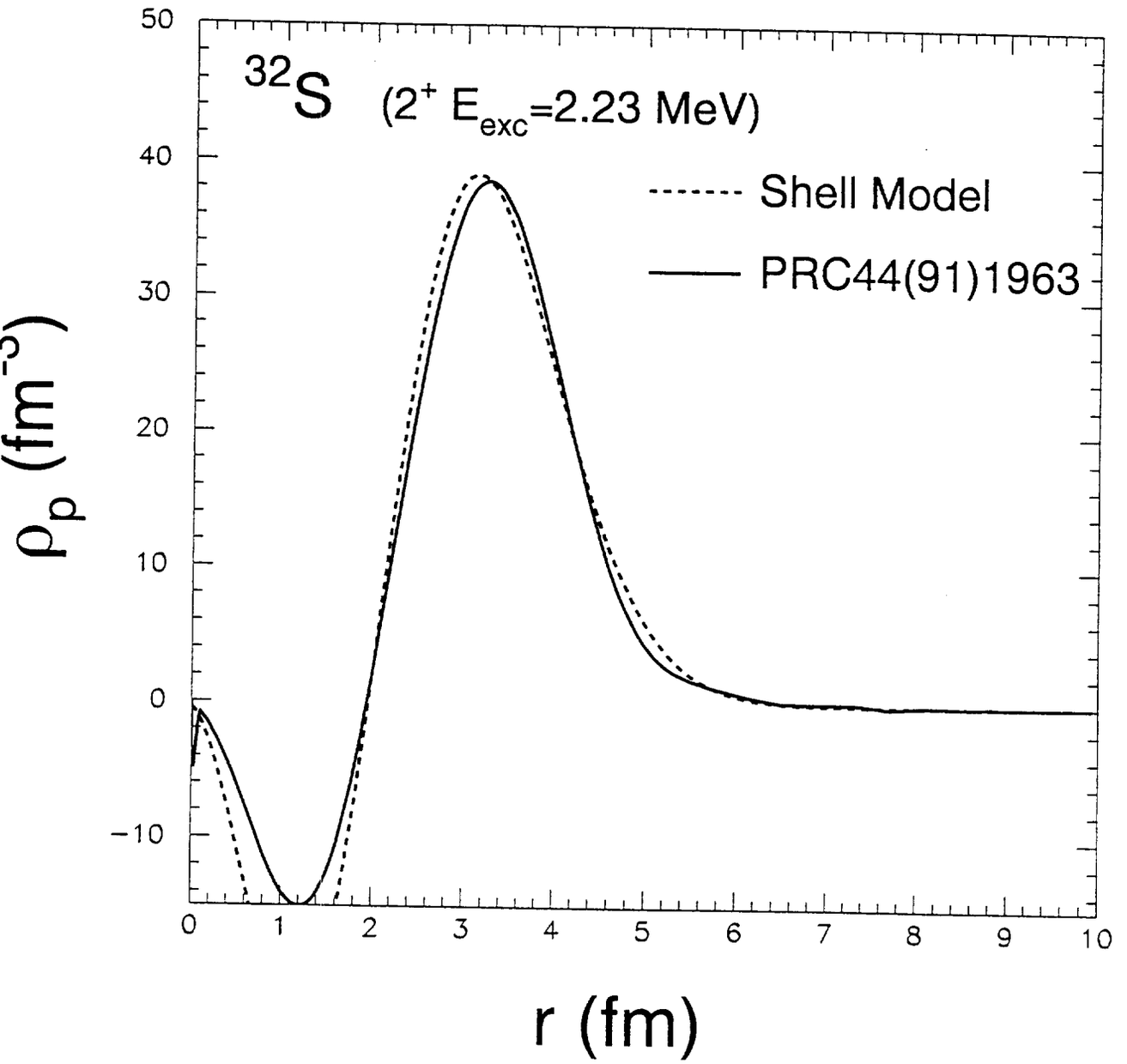
^{32}S
(2^+ E_{exc}=2.23 MeV)
Shell Model
PRC44(91)1963
ρ_p (fm^{-3})
r (fm)
50
40
30
20
10
0
−10
0
1
2
3
4
5
6
7
8
9
10

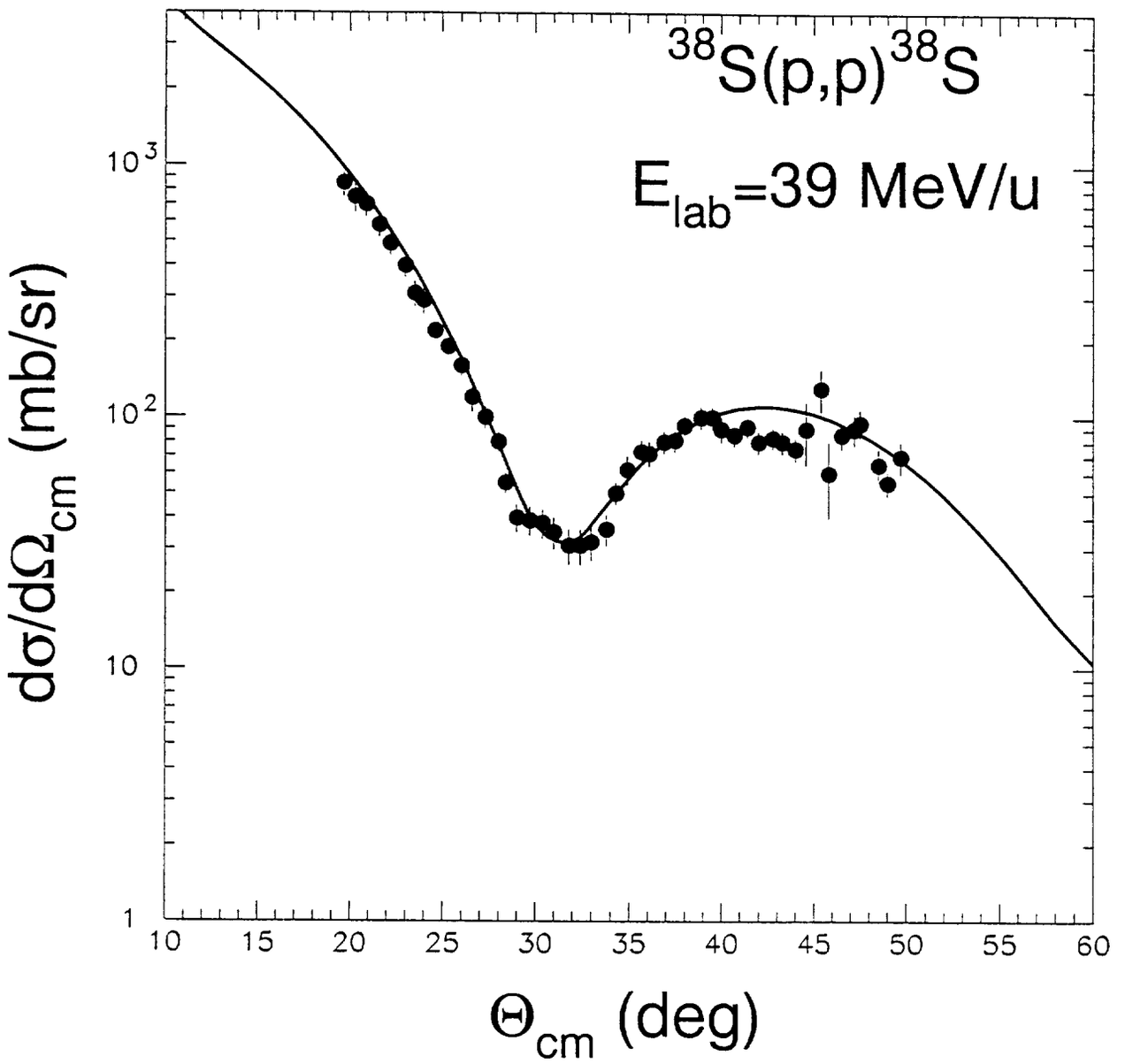
$^{38}S(p,p)^{38}S$
E_{lab}=39 MeV/u
$d\sigma/d\Omega_{cm}$ (mb/sr)
Θ_{cm} (deg)
10^3
10^2
10
1
10
15
20
25
30
35
40
45
50
55
60

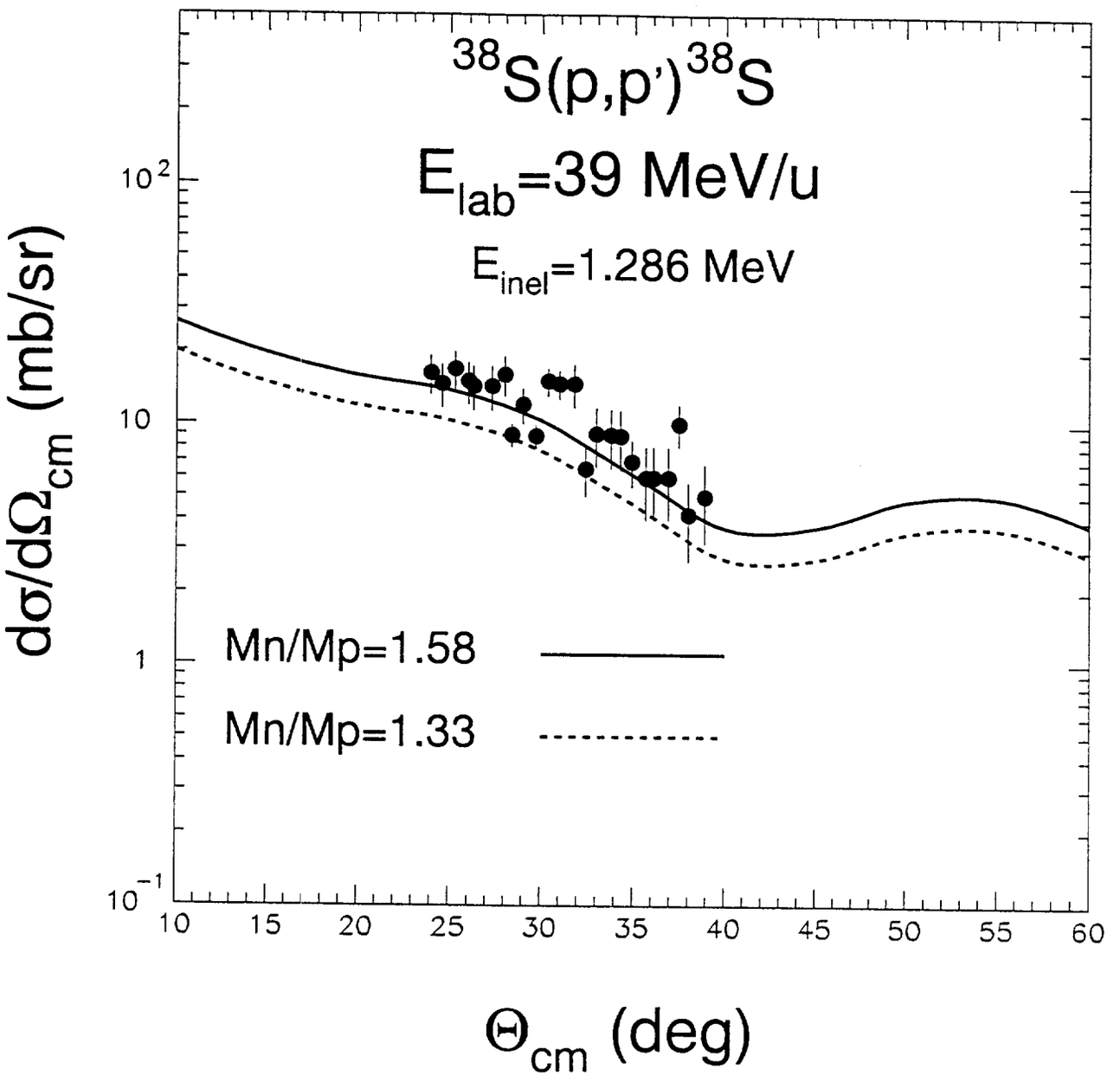
$^{38}S(p,p')^{38}S$
E_{lab}=39 MeV/u
E_{inel}=1.286 MeV
Mn/Mp=1.58
Mn/Mp=1.33
$d\sigma/d\Omega_{cm}$ (mb/sr)
Θ_{cm} (deg)
10^2
10
1
10^{-1}
10
15
20
25
30
35
40
45
50
55
60

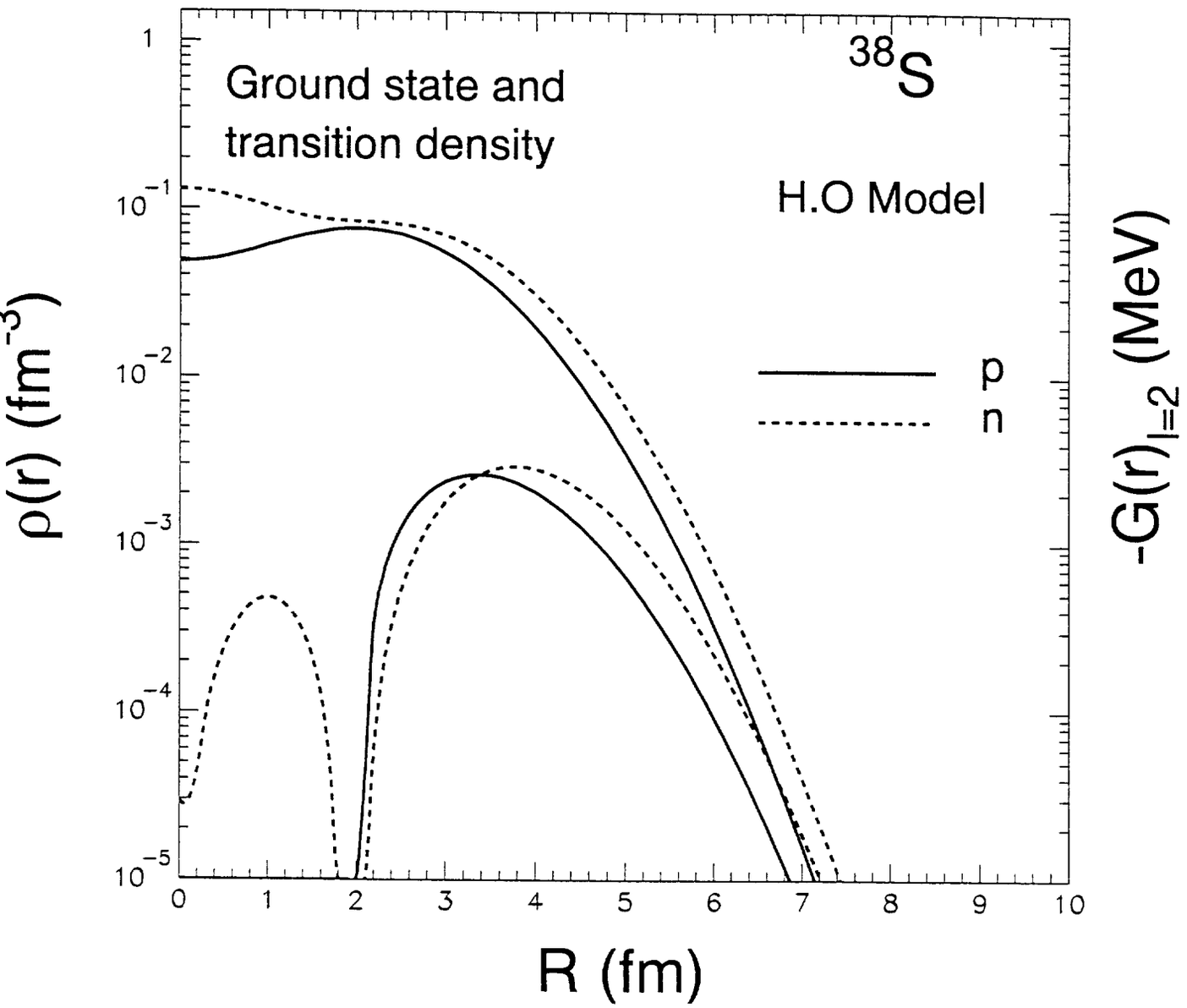
Ground state and
transition density
^{38}S
H.O Model
p
n
ρ(r) (fm^{-3})
-G(r)$_{l=2}$ (MeV)
R (fm)
1
10^{-1}
10^{-2}
10^{-3}
10^{-4}
10^{-5}
0
1
2
3
4
5
6
7
8
9
10